

Simulation of a non-ideal saddle coil on toroidally symmetric magnetic confinement experiments.

RALPH EWIG, THOMAS R. JARBOE

University of Washington, PO Box 352250, Seattle, Washington 98195

Abstract

A method for modeling the time varying magnetic geometry in a low aspect ratio tokamak is developed. The model includes mutual inductance effects of an arbitrarily shaped (toroidally symmetric) conducting shell, poloidal field coils, a saddle coil with finite gap resistance, and a single element, distributed plasma current. The plasma current distribution is specified using EFIT results, and remains unchanged during the simulation, while the magnitude of the plasma current is ramped up linearly over time. The resulting simulation code is used to predict power supply requirements and tracking capabilities of an arbitrarily chosen feedback mechanism employed to operate the poloidal field coils of the tokamak.

Simulation of a non-ideal saddle coil on toroidally symmetric magnetic confinement experiments.

RALPH EWIG, THOMAS R. JARBOE

University of Washington, PO Box 352250, Seattle, Washington 98195

Introduction

The University of Washington in collaboration with the Princeton Plasma Physics Laboratory has proposed a three-year program to study Coaxial Helicity injection (CHI) on the National Spherical Torus Experiment (NSTX) as a method of formation and sustainment of a spherical tokamak. CHI is a steady state method of current drive that does not require a transformer and is compatible with low aspect ratio tokamaks¹. The Helicity Injected Torus (HIT) experiment at the University of Washington has achieved plasma currents of up to 250kA with an injector current of about 20kA in a low aspect ratio ($A=1.5$) geometry². On NSTX it is planned to use CHI to startup the spherical tokamak (ST) and to sustain the edge plasma during sustained operation. In order to determine whether or not the power supplies intended for use on NSTX will be capable of maintaining desirable flux boundary conditions throughout the discharge, a computational model of the time varying magnetic field geometry has been developed. The model includes mutual inductance effects of an arbitrarily shaped conducting shell, poloidal field coils, a saddle coil with finite gap resistance, and a single element, distributed plasma current. The plasma current distribution is specified and remains unchanged during the simulation, while the total magnitude of the plasma current is ramped up linearly over time. In addition, the interaction of the poloidal field coil flux feedback mechanism with the passive elements of the experiment is included. Given the geometry of the experiment, a mechanism for feedback control of the poloidal field coils, a specified plasma current, and desired flux boundary conditions, the model should return the currents versus time in all elements.

Similar calculations have been performed for the HIT-II experiment at the University of Washington.³ However, HIT-II does not include a saddle coil in its design thus considerably simplifying the problem. While calculations of the magnetic field effects of saddle coils on tokamaks have been

studied⁴, the simulation of a saddle coil in combination with flux feedback control on a CHI driven tokamak poses a previously unaddressed problem.

This paper presents a mathematical methodology, which allows modeling the given problem with a non-iterative, time-stepping method. All conducting elements on the experiment are assumed to be toroidally symmetric. The model determines the currents in all conducting elements at each time step, and once the currents are known, the magnetic flux geometry is easily determined using a toroidally symmetric, circular filament model to calculate the required green-functions.⁵

Development of Time-Varying Equations

The simulation code models the interaction between all conducting material elements on the experiment, assuming toroidal symmetry in all elements. There are 4 different element types which are considered:

1. vessel elements (passive)
2. driven coils (active)
3. saddle coil elements (passive)
4. plasma current (modeled as a single, distributed driven coil equivalent to item 2 - active)

Once the currents in all these elements are known, the resulting flux can be calculated using previously determined green-functions for all desired locations, and a distributed spatial grid. The plasma current distribution is taken from EFIT results and remains unchanged during the simulation. The total plasma current is increased linearly over time to simulate the effect of a CHI driven plasma. Once the green functions for the plasma distribution acting at the locations of the flux loops and the spatial grid have been determined, it can be treated as a single coil. The plasma is then treated as a current feedback driven coil, with the demand set to the desired value at each time step. This leaves us with three remaining subcategories. The saddle coil elements are described as 'non-ideal', in the sense that the resistance across the gap is finite, rather than infinite as would be the case with an ideal saddle-coil (compare Figure 1). In

the case of NSTX, the 'insulating' material constituting the gap of the saddle coil is stainless steel, whereas the remainder is made of copper.

Consider the general current element shown in Figure 2 as a representation of all three subclasses. Each of the cases can then be recovered by adjusting the properties of the general circuit:

1. Vessel-element: $\tilde{R} = 0, \tilde{V} = 0, R \neq 0, V \neq 0$
2. Driven-Coil: $\tilde{R} = \infty, \tilde{V} \neq 0, R \neq 0, V \neq 0$
3. Saddle Coil: $\tilde{R} \neq 0, \tilde{V} \neq 0, R \neq 0, V \neq 0$

The equivalent circuit diagram for the general current element is shown in Figure 3. To find the current generated by the two time-varying DC voltage sources, each voltage source is treated as the sole source in the circuit with the other replaced by a short, and the results are then super-imposed.⁶ The resulting expression for the current is:

$$IR = V - \tilde{V} \quad (1)$$

V is the voltage due to self and mutual inductance. Defining M as a matrix that contains the mutual inductance values for elements i and j, the induced voltage for the i-th current element it is given by⁷:

$$V_i = -\dot{\Phi}_i = -L \frac{dI_i}{dt} - \sum_{\substack{j=1 \\ j \neq i}}^n \left(M_{ij} \frac{dI_j}{dt} \right) = -\sum_{j=1}^n (M_{ij} \dot{I}_j) \quad (2)$$

The expression for the total current in the element then becomes:

$$(IR)_i = -\sum_{j=1}^n (M_{ij} \dot{I}_j) - \tilde{V}_i \quad (3)$$

Make the following definitions for convenience of notation:

$$\frac{M_{ij}}{R_i} = \tau_{ij} \quad \tilde{I}_i = \frac{\tilde{V}_i}{R_i} \quad (4)$$

The resulting equation for the currents in all the elements is then:

$$\vec{I} = -\vec{\tau} \cdot \vec{I} - \vec{\tilde{I}} \quad (5)$$

It is easily determined that the solution to this set of ordinary differential equations is given by⁸:

$$\vec{I}(t) = e^{-\tau^{-1} \cdot (t-t_0)} \left(\vec{I}_0 + \vec{\tilde{I}}_0 \right) - \vec{\tilde{I}} \quad (6)$$

Where the operation $\tau^{-1}(t-t_0)$ is defined as taking the inverse of the matrix τ and then multiplying each element of the resulting matrix with the size of the time-step. The only difference between different element types is in the term for $\vec{\tilde{I}}$. In order to utilize equation 8 in a computational simulation it needs to be discretized over each time-step, where the voltage ($\vec{\tilde{R}}_i$) is held constant over the time-step:

$$\vec{I}_{j+1} = e^{-\tau^{-1} \cdot \Delta t} \left(\vec{I}_j + \vec{\tilde{I}}_{j+1} \right) - \vec{\tilde{I}}_{j+1} \quad (7)$$

The external voltage represented by the $\vec{\tilde{I}}$ term is due either to an applied voltage from a power supply or from the inter-connections of individual current elements that are part of the saddle coil. In the first case, $\vec{\tilde{I}}$ is simply the voltage put out by the power supply divided by the resistance R of the current element under consideration. For saddle coil elements, the determination of $\vec{\tilde{I}}$ involves another calculation. As defined previously $\vec{\tilde{V}}$ is the voltage across the resistor $\vec{\tilde{R}}$. Figure 4 illustrates how the value of $\vec{\tilde{V}}$ for a saddle coil element is determined by the equivalent resistance of the combined material making up the gap of the saddle coil, and the currents in each individual saddle element. Consequently, the contribution to the voltage from the saddle is given by:

$$\vec{\tilde{V}}_{\text{saddle}} = R_{\text{eq}} \cdot \sum I_i \quad (8)$$

The sum is performed over saddle coil elements only. In order to find a general expression, a binary vector (\vec{a}) is defined that contains the value 1 for a saddle coil element and 0 for all other elements. The current $\vec{\tilde{I}}$ can then be expressed as follows:

$$\vec{\tilde{I}} = (\vec{a} \cdot \vec{I}) \cdot \left(\frac{\vec{R}_{eq}}{R_i} a_i \right) + \left(\frac{\vec{V}_i^{app}}{R_i} \right) \quad (9)$$

Where V^{app} is zero for all passive elements that are not connected to a power-supply. The resulting expression for the current is given by:

$$\vec{I}_{j+1} = e^{-\tau^{-1}\Delta t} \left[\vec{I}_j + (\vec{a} \cdot \vec{I}_{j+1}) \cdot \left(\frac{\vec{R}_{eq}}{R_i} a_i \right) + \left(\frac{\vec{V}_i^{app}}{R_i} \right)_{j+1} \right] - (\vec{a} \cdot \vec{I}_{j+1}) \cdot \left(\frac{\vec{R}_{eq}}{R_i} a_i \right) - \left(\frac{\vec{V}_i^{app}}{R_i} \right)_{j+1} \quad (10)$$

This can further be simplified as follows:

$$\vec{I}_{j+1} = e^{-\tau^{-1}\Delta t} \left[\vec{I}_j + \left(\frac{\vec{V}_i^{app}}{R_i} \right)_{j+1} \right] - \left(\frac{\vec{V}_i^{app}}{R_i} \right)_{j+1} + (e^{-\tau^{-1}\Delta t} - \vec{I}) (\vec{a} \cdot \vec{I}_{j+1}) \cdot \left(\frac{\vec{R}_{eq}}{R_i} a_i \right) \quad (11)$$

$$\vec{I}_{j+1} = e^{-\tau^{-1}\Delta t} \underbrace{\left[\vec{I}_j + \left(\frac{\vec{V}_i^{app}}{R_i} \right)_{j+1} \right]}_{\vec{b}} - \left(\frac{\vec{V}_i^{app}}{R_i} \right)_{j+1} + \underbrace{(\vec{a} \cdot \vec{I}_{j+1}) (e^{-\tau^{-1}\Delta t} - \vec{I})}_{\vec{c}} \cdot \left(\frac{\vec{R}_{eq}}{R_i} a_i \right) \quad (12)$$

This expression is then solved for the current I ($j+1$):

$$\begin{aligned} \vec{I} &= (\vec{a} \cdot \vec{I}) \cdot \vec{c} + \vec{b} \\ \vec{I} - (\vec{a} \cdot \vec{I}) \cdot \vec{c} &= \vec{b} \\ \Rightarrow \vec{S} \cdot \vec{I} &= \vec{b} \\ \mathbf{S}_{ij} &= (\delta_{ij} - c_i a_j) \end{aligned} \quad (13)$$

Re-substitution of the previous simplifications yields the final expression for the currents at each given time-step:

$$\vec{I}_{j+1} = \vec{S}^{-1} \left[e^{-\tau^{-1}\Delta t} \left(\vec{I}_j + \left(\frac{\vec{V}_i^{app}}{R_i} \right)_{j+1} \right) - \left(\frac{\vec{V}_i^{app}}{R_i} \right)_{j+1} \right] \quad (14)$$

If no saddle coil is present, the matrix S (and therefore its inverse) degenerate into the identity matrix.

Results

In order to test the model for physical validity, a number of special cases can be utilized, using a simplified geometry on the experiment. In all of the following cases, the expected results are easily determined:

1. Infinite gap-resistance in a non-symmetric magnetic field geometry, resulting in equal and opposite currents in the two halves of the saddle coil.
2. Infinite gap-resistance with the magnetic field symmetric across the midplane of the experiment. In this case no current should be observed in the saddle coil at all.
3. Finite gap-resistance in a non-symmetric magnetic field. The flux just inside of the two halves of the saddle coil should be identical.
4. Finite gap-resistance with the magnetic field symmetric across the midplane of the experiment. The currents in both halves of the saddle coil should be identical and decay on a L/R time scale of the gap resistance.

All of these test cases were run using a simplified saddle coil geometry of the NSTX experiment, and a trapezoidal shape for the flux demand function. The demanded flux is specified at the location of the actively driven coil, and its value is ramped from zero to twenty milli-webers in the time from negative ten to zero milli-seconds. All flux contour plots are shown after the maximum value has been reached and held constant for at least ten milli-seconds. Figure 5 shows the magnetic flux geometry for case 1, looking at a poloidal cross-section of the experiment with the major axis at the zero r coordinate. The currents in the saddle for this case are shown in Figure 6. The solid line indicates the current flowing through the gap of the saddle coil, which is zero in this case. The dashed and dotted-dashed lines show the currents in the upper and lower half of the saddle coil. The currents in case number two are identically zero (no plot is shown). The accompanying magnetic flux geometry is shown in Figure 7.

For cases three and four the resistance in the gap of the saddle coil was changed to $300\mu\Omega$. The currents through the gap and each half of the saddle coil in case three are shown in Figure 8. The currents for the fourth case are shown in Figure 9.

Figure 10 shows a simulation of the entire NSTX experiment, including a distributed plasma current with a peak value of 810 kAmps⁹. The entire distribution is ramped from zero to the maximum value over a time span of 10 milliseconds. The plot shows the magnetic flux geometry at 10 milliseconds after the plasma current has reached its peak value.

Discussion

As expected, in the cases of infinite gap resistance (case 1 & 2), the current through the gap of the saddle coil is identically zero. In case one where the magnetic field is non-symmetric, this results in equal and opposite currents in the upper and lower halves of the saddle coil as shown in Figure 6. The magnetic flux geometry for this case clearly exhibits the saddle coil's tendency to equalize the magnetic flux values between the upper and lower halves of the coil (Figure 5). In the second case where a symmetric magnetic field is applied, all currents are zero and the magnetic flux passes right through the saddle coil as if it were a non-conductor (Figure 7).

After setting the gap resistance to a finite value, the third case shows the current through the gap is no longer zero and decays on the L/R time-scale (Figure 8). The currents in the upper and lower halves can be observed to decay on a longer time-scale due to the lower resistance of the saddle coil material in comparison to the gap. However, the sum of the two (which is identical to the gap current) goes to zero much faster, on the gap resistance L/R time.

In case four (symmetric field with finite gap resistance) the upper and lower halves of the saddle coil carry exactly identical currents, and all currents decay on the L/R time-scale of the gap material. Again this is as expected for a symmetric magnetic field geometry. Lastly, the simulation of the entire NSTX experiment (Figure 10) illustrates the methods capability to include contributions from passive elements as well as the distributed plasma current.

Summary

A method for modeling the time varying magnetic geometry in a toroidally symmetric geometry was developed. The model includes mutual inductance effects of an arbitrarily shaped conducting shell, poloidal field coils, a saddle coil with finite gap resistance, and a single element, distributed plasma current. Results from simulations of four special cases show the model to perform as predicted from physical arguments. Additional results of a simulation of the National Spherical Torus Experiment (NSTX) are shown, demonstrating the model's capability to include the effects of a distributed plasma current.

The resulting simulation code is a useful tool to predict power supply requirements for the poloidal field coils of any toroidally symmetric magnetic confinement device. Since the underlying mathematics do not specify in what way the voltage is generated which is applied to active elements, any desired method of feedback control (current feedback, flux feedback, pulse width modulation, etc.) can easily be implemented. By adding the particular characteristics of the experiment hardware to the basic model, any type of power supply can be evaluated for the given task.

In its present form the model does not include the resistance from the connections of one half of the saddle coil to another. In the case of the original problem of modeling NSTX it was possible to neglect these effects. Depending on the geometry under consideration this might become important and require appropriate adjustments of the model.

Acknowledgements

The author would like to acknowledge Dr. Dave Orvis whose contributions of similar simulations on the HIT-II experiment initiated the work presented in this paper. In addition, the author would like to thank Prof. Brian Nelson, Prof. Uri Shumlack, Karsten McCollam, and Dr. Roger Raman at the University of Washington; as well as Dr. Stan Kaye from the Princeton Plasma Physics Laboratory.

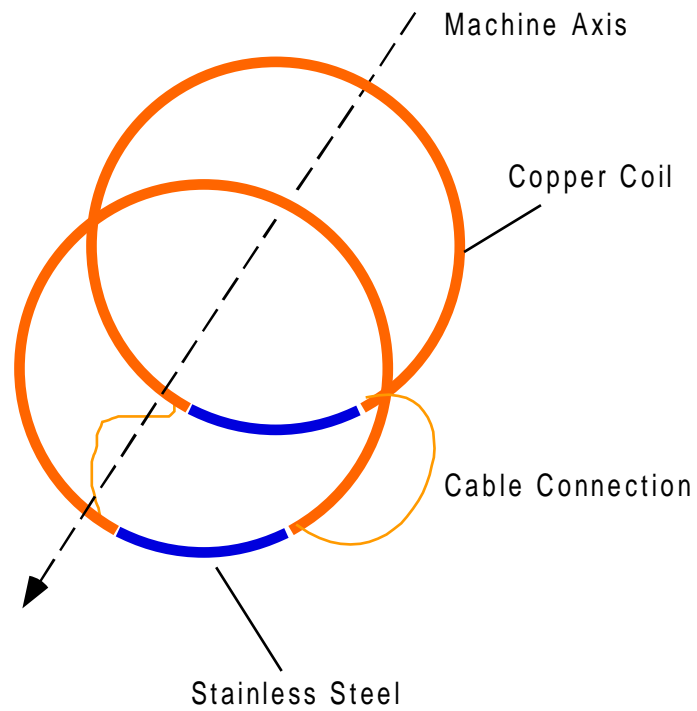


Figure 1: Schematic of the NSTX non-ideal saddle coil. The 'insulating' gap of the saddle-coil is made of stainless steel.

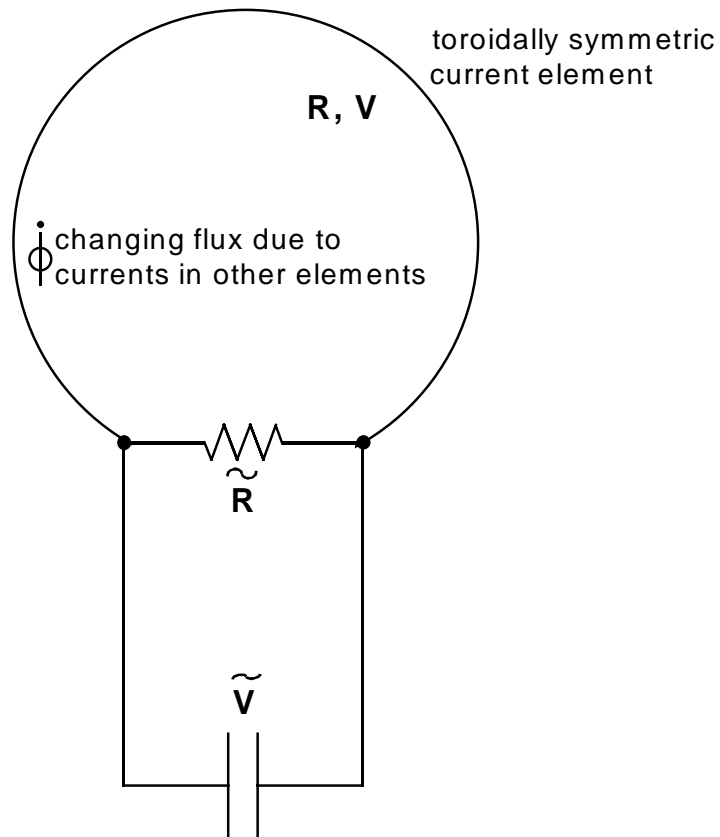


Figure 2: Schematic of the general current element model.

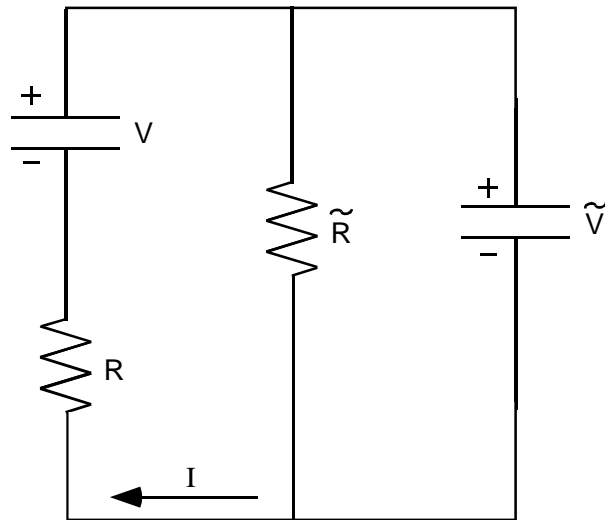


Figure 3: Circuit diagram for a general current element.

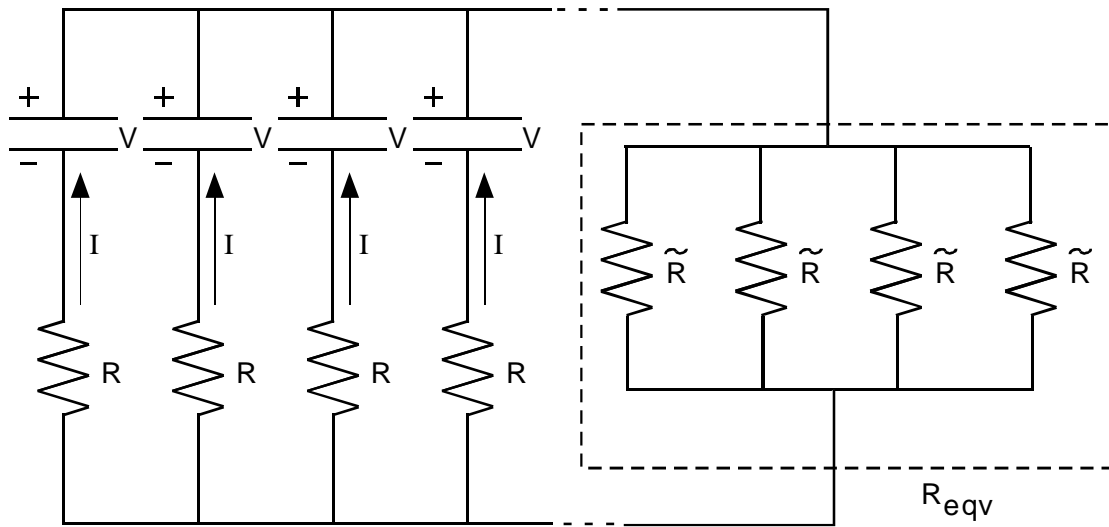


Figure 4: Circuit of equivalent gap resistance.

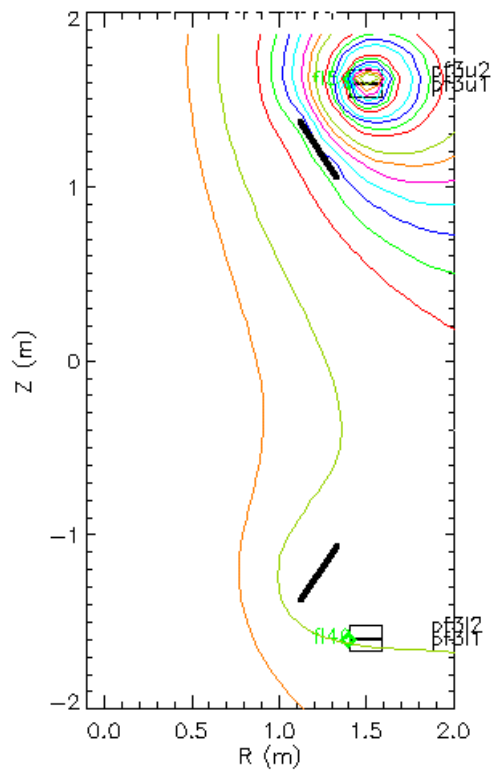


Figure 5: Magnetic flux geometry for infinite gap resistance and non-symmetric field.

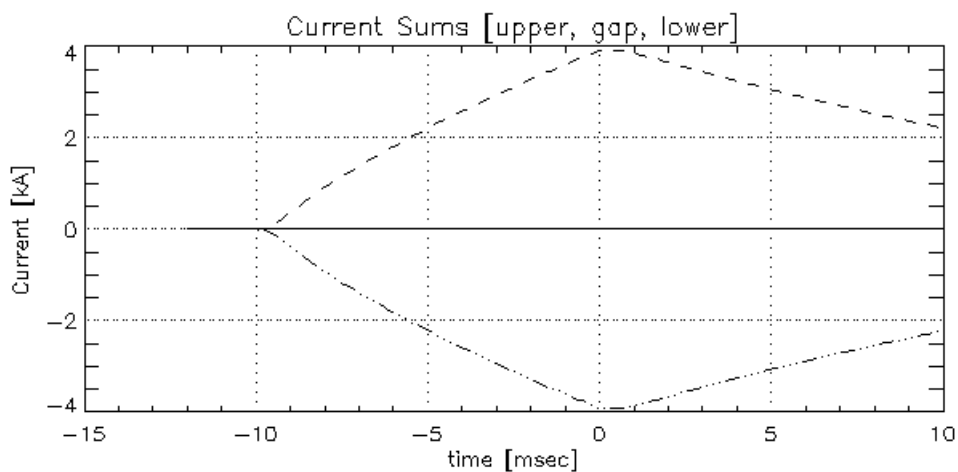


Figure 6: Currents for infinite gap resistance in the saddle coil and a non-symmetric magnetic field.

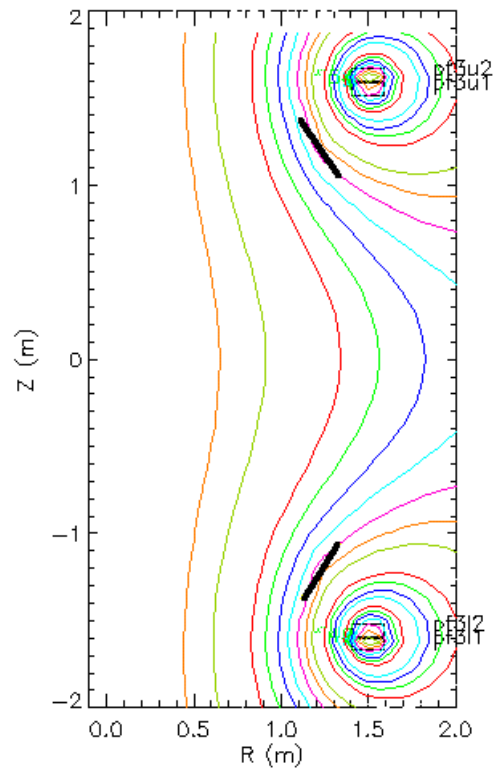


Figure 7: Magnetic flux geometry for infinite gap resistance and symmetric field.

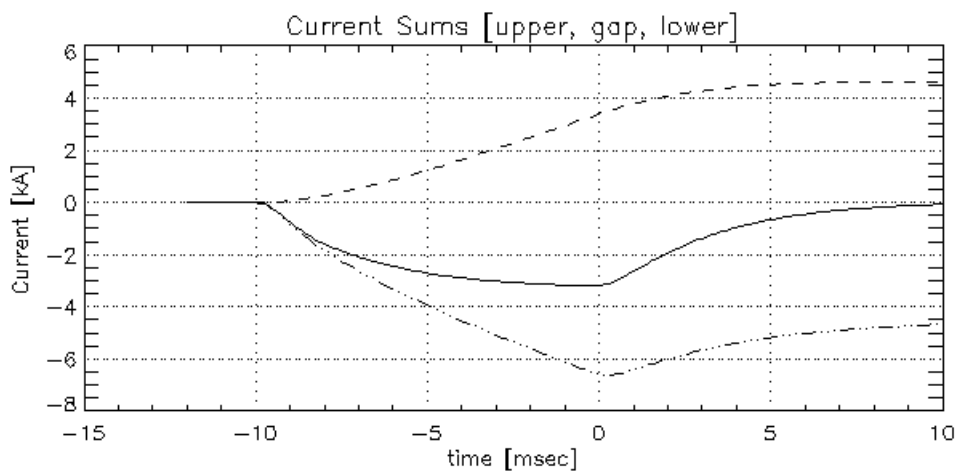


Figure 8: Current plots for finite gap resistance and a non-symmetric magnetic field.

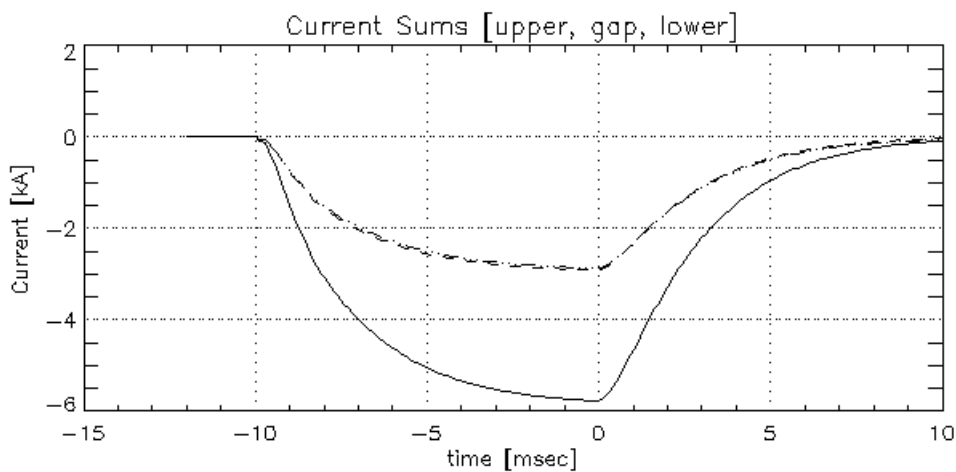


Figure 9: Current plots for finite gap resistance and a midplane-symmetric magnetic field.

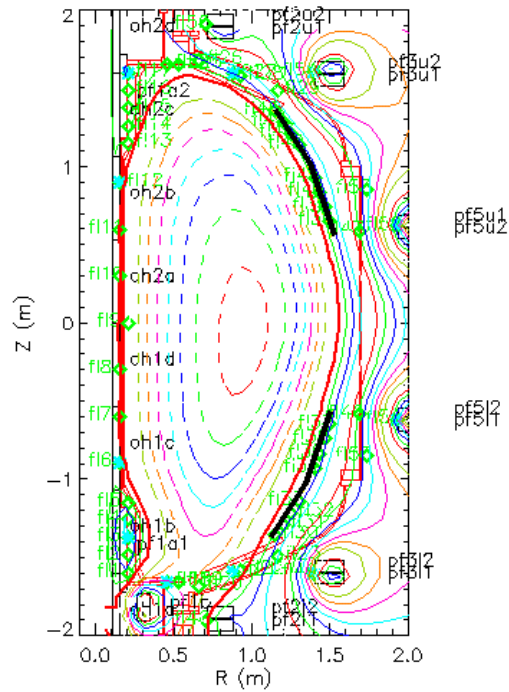


Figure 10: Magnetic Flux plot for 810 kAmps plasma current simulation in NSTX. In this case the poloidal field coils are feedback controlled by the flux measured at various locations on the experiment to obtain constant flux boundary conditions. The resulting magnetic flux geometry is typical for a CHI driven, low-aspect ratio tokamak.

Bibliography

¹ T. R. Jarboe, "Formation and steady-state sustainment of a tokamak by coaxial helicity injection.", *Fusion Technology*, **15**, 7 (1989).

² B. A. Nelson, T.R. Jarboe, D J. Orvis, L. McCullough, J. Xie, C. Zhang, and L. Zhou, *Phys. Rev. Lett.* **72**, 3666 (1994).

³ D. J. Orvis, personal communications, University of Washington, HIT Plasma Physics group, 1997

⁴ N. I. Doinikov, "Magnetic field of saddle-shaped shell coils", *Soviet Physics - Technical Physics*, vol.28, no.11, pp. 1407, 8. Nov. 1983.

⁵ Jackson, J. D., "Classical Electrodynamics", 2nd Edition, Wiley & Sons, NY, 1975, pp.177

⁶ D. E. Johnson, *et al*, "Basic Electric Circuit Analysis", 5th Edition, 1995, Prentice-Hall, pp.198.

⁷ D. J. Griffiths, "Introduction to Electrodynamics", 2nd Edition, 1989, Prentice-Hall, pp. 293

⁸ E. Kreyszig, "Advanced Engineering Mathematics", 7th Edition, 1993, Wiley & Sons, pp. 186

⁹ S. Kaye et al, "Physics Design of the National Spherical Torus Experiment", submitted for publication in *Fusion Technology*, 1998